

## ENGINEERING

# A wearable textile-based pneumatic energy harvesting system for assistive robotics

Rachel A. Shveda<sup>1†</sup>, Anoop Rajappan<sup>1†</sup>, Te Faye Yap<sup>1</sup>, Zhen Liu<sup>1</sup>, Marquise D. Bell<sup>1</sup>, Barclay Jumet<sup>1</sup>, Vanessa Sanchez<sup>2,3</sup>, Daniel J. Preston<sup>1\*</sup>

Wearable assistive, rehabilitative, and augmentative devices currently require bulky power supplies, often making these tools more of a burden than an asset. This work introduces a soft, low-profile, textile-based pneumatic energy harvesting system that extracts power directly from the foot strike of a user during walking. Energy is harvested with a textile pump integrated into the insole of the user's shoe and stored in a wearable textile bladder to operate pneumatic actuators on demand, with system performance optimized based on a mechano-fluidic model. The system recovered a maximum average power of nearly 3 W with over 20% conversion efficiency—outperforming electromagnetic, piezoelectric, and triboelectric alternatives—and was used to power a wearable arm-lift device that assists shoulder motion and a supernumerary robotic arm, demonstrating its capability as a lightweight, low-cost, and comfortable solution to support adults with upper body functional limitations in activities of daily living.

## INTRODUCTION

More than 30 million adults in the United States live with an upper body functional limitation (1). The most common limitation reported among adults is difficulty lifting a 4.5-kg object, with 13 million unable to do so at all, while several million adults also have difficulty grasping, reaching, and pushing or pulling with their hands (1). Upper body function is critical to a person's ability to perform activities of daily living such as eating, dressing, and bathing; limited ability to perform these functions correlates with an increased risk of mortality (2), and employed adults with a disability earn 25% less than adults without a disability (1). Wearable assistive devices that are soft, affordable, low profile, lightweight, and portable can substantially enhance pathways to recovery and quality of life for individuals with upper body impairments (3, 4).

Various assistive and rehabilitative devices have been designed to support individuals with upper body limitations; these devices include soft exogloves for hand support and rehabilitation (5–7), exosuits for back support and rehabilitation (8, 9), and exosleeves for shoulder (10–12), elbow (13–15), forearm (16, 17), and wrist (18–20) support and rehabilitation (21, 22). These devices can also serve to augment the capabilities of nondisabled adults by, for example, acting as a supernumerary limb (or “third arm”) (23–27), supplementing lifting capacity (28), or providing hip and ankle assistance during loaded walking (29, 30). Supernumerary robotic limbs, in particular, have been effective in supporting, assisting, or enhancing users' existing capabilities (31–34). Wearable robotic devices are often made from soft and lightweight materials such as elastomers and textiles to promote comfort and safety of the user (3). However, these devices require power, and the weight and bulk of common power supplies such as batteries, compressors, and pumps, as well as accompanying hardware such as valves, cables, and electronics, often make these tools more of a burden than an

asset (35). The development of lightweight, portable, and unobtrusive power sources is thus a prerequisite for the emergence of practical wearables that fully leverage the capabilities of soft robotic actuators (35, 36).

Integration of energy harvesting capability in clothing offers an attractive substitute for bulky onboard power units and is capable of substantially reducing device weight and size while precluding the need for recharging or refueling as power is generated continuously during use. Body movement, heat, and biochemical potential are all readily available and easily accessible energy sources for wearable devices, with motion of the limbs—specifically, foot strike—representing the most abundant source of power (37–39). Shoe-based energy harvesting systems have been developed to capitalize on this source of power since as early as 1948 (40, 41). Several physical mechanisms have been used to harvest energy during walking: pneumatic, electromagnetic, triboelectric, piezoelectric, hydroelectric, thermo-electric, and pyroelectric approaches have been demonstrated in prior work (38, 39). Recently, advances in thin-film and fiber-based triboelectric nanogenerators and fiber lithium-ion batteries have enabled their direct integration into shoe insoles and woven textiles (42–44). However, the power output of these devices is currently in the milliwatt range, which, although suitable for sensors and low-power electronics, remains inadequate for powering practical assistive actuators during everyday use. In addition, because many soft actuators used in assistive devices rely on pneumatic actuation (5, 45, 46), approaches that generate electricity require an additional conversion step from electrical to pneumatic power for use with these assistive devices, further reducing efficiency and adding bulk by requiring more components (47, 48). Ogawa *et al.* (49, 50) developed an in-shoe pneumatic energy harvesting system, but still relied on a hard tank for pneumatic energy storage; furthermore, their system was neither modeled to elucidate the underlying physics and thermodynamics of operation nor optimized for maximum performance.

In this work, we develop a textile-based energy harvesting system that extracts pneumatic energy using a soft textile pump integrated directly into the insole of the user's shoe; the energy harvested during walking is stored inside a soft, wearable textile bladder until

Copyright © 2022  
The Authors, some  
rights reserved;  
exclusive licensee  
American Association  
for the Advancement  
of Science. No claim to  
original U.S. Government  
Works. Distributed  
under a Creative  
Commons Attribution  
NonCommercial  
License 4.0 (CC BY-NC).

<sup>1</sup>Department of Mechanical Engineering, William Marsh Rice University, Houston, TX 77005, USA. <sup>2</sup>John A. Paulson School of Engineering and Applied Sciences, Harvard University, Cambridge, MA 02138, USA. <sup>3</sup>Wyss Institute for Biologically Inspired Engineering, Harvard University, Boston, MA 02115, USA.

\*Corresponding author. Email: djp@rice.edu

†These authors contributed equally to this work.

dispensed by the user to power actuators as needed. Our energy harvesting platform thus enables users to comfortably produce and store the power needed to operate the pneumatic actuators found in many common assistive and rehabilitative devices. We built our devices using stacked laminate assembly of heat-sealable textiles, ensuring scalability and ease of manufacturing (3, 36). To optimize the performance of our system, we developed a mechano-fluidic model, validated its predictions against experimental results, and used it to guide the final design of our devices. Our system achieved high conversion efficiencies, recovering more than 20% of the mechanical energy available from walking during experiments; the insole textile pump attained a maximum average power output of 3 W that surpasses the capabilities of existing foot-strike energy harvesting systems based on electrical mechanisms. The direct generation of pneumatic power further eliminates the need for an additional electric-to-pneumatic energy conversion step required by alternate approaches. We demonstrate the use of our system in powering two assistive actuators fabricated entirely from textiles: (i) an arm-lift device that assists shoulder motion and (ii) a robotic “third arm” that augments user capability.

## RESULTS

### The textile-based pneumatic energy harvesting system

The soft energy harvesting system comprises two key components each built from textiles: an insole pneumatic pump, which we call the “energy harvesting device” or EHD, and a wearable pneumatic accumulator, which we refer to as the “energy storage bladder” or ESB (Fig. 1). Both the EHD and the ESB were fabricated by first

laser patterning and then thermally bonding layers of heat-sealable textile, namely, nylon taffeta fabric coated on one side with thermoplastic polyurethane (TPU). Our fabrication approach was guided mainly by the need for scalability and ease of manufacturing of our textile devices; laser patterning allows fast and easy customization of devices, and heat sealing of thermoplastic-coated fabric is a widely adopted technique in the commercial production of garments (51). Stacked laminate assembly of carefully designed textile layers yielded durable insole EHDs capable of enduring large applied forces (~300 N) and cyclic deformation, and a wearable, low-profile ESB capable of storing air at high pressure (~1 bar) with no leakage.

During walking, the compressive force exerted by the user’s foot performs mechanical work on the EHD; the EHD converts this work into free energy of pressurized gas, which is then conveyed to and stored in the ESB for later use. To enable its operation as an air pump, we filled the textile pouch of the EHD with water-blown polyurethane foam (Fig. 1A) and added a pair of check valves to enforce unidirectional flow of air from the inlet to the outlet (52) (Fig. 1C). When force applied by the foot depresses the EHD (the “foot strike” or compression phase of the pump cycle), air within the pouch is pressurized and forced through the outlet valve into the ESB. When the foot is raised, relieving the force on the EHD (the “liftoff” or intake phase of the pump cycle), the pouch inflates under the restoring force of the foam and is refilled by ambient air drawn through the inlet valve. We fabricated three different prototypes of the EHD, with pouch volumes of 6, 35, and 72 ml; other aspects of the design were kept unchanged. Figure 1C illustrates one possible configuration of the energy harvesting system and the corresponding placement of the EHD and ESB on the user: The

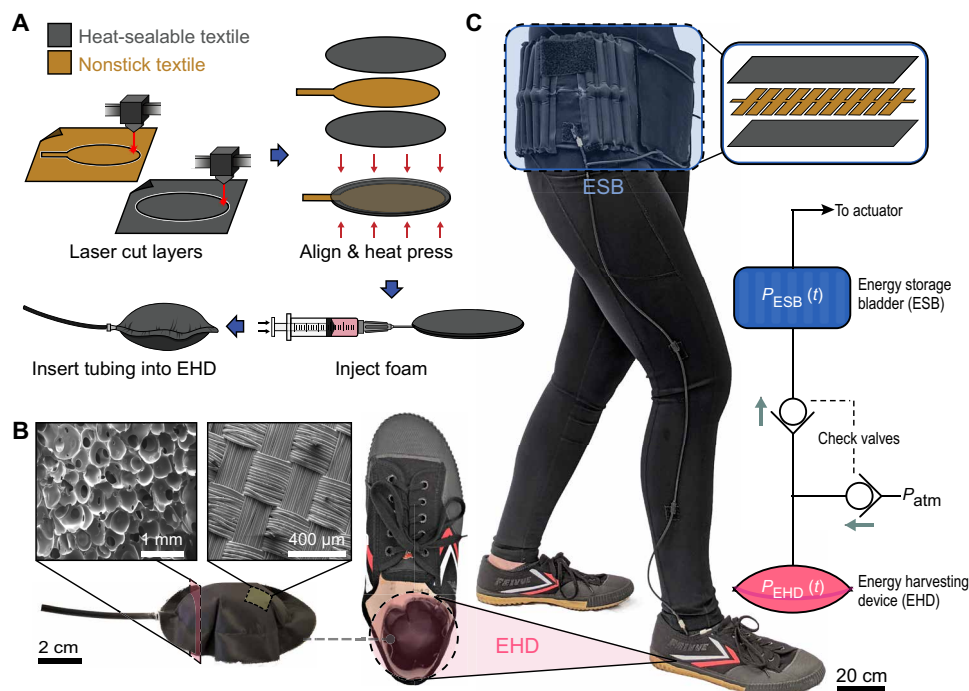


**Fig. 1. Fabrication and donning of the textile-based energy-harvesting system.** (A) Fabricating the insole EHD from heat-sealable textile layers. (B) Scanning electron micrographs of EHD components: open-cell foam interior and textile exterior. (C) A user wearing the fully assembled system. The EHD is integrated into the insole of the right shoe, and the textile ESB is worn around the waist. Insets show the textile layers used to fabricate the ESB and a schematic diagram of the pneumatic circuit linking the EHD and ESB.

flexible ESB may be worn comfortably around the user's waist, and the soft EHD fits unobtrusively inside the user's shoe. The ESB serves as a portable source of pressurized air for powering pneumatic actuators that assist the user with various functions. The ESB can be repositioned easily, without affecting system performance, to enhance comfort or facilitate use with commercial assistive and rehabilitative pneumatic devices.

To evaluate the performance of our energy harvesting system, we measured the force of foot strike on the EHD and the pressure inside the ESB as a function of time for a 55-kg user walking on a treadmill at 3 mph (4.8 km/hour, corresponding to the average walking speed for adults less than 30 years old) (53), as shown in Fig. 2A. A video recording of the test using the 35-ml EHD is included as movie S1. The system successfully extracted and stored pneumatic energy during walking, which was subsequently used to power two textile-based actuators, namely, a soft arm-lift assistive device and a supernumerary arm.

### Mechano-fluidic modeling of the textile energy harvesting system

We used a quasi-static force balance on the pouch to model fluid flow through the EHD and thereby characterize its pumping performance (Fig. 2B). To simplify analysis, air inside the pouch was modeled using the ideal gas equation of state, and the temperature of the gas was assumed constant and equal to the steady-state temperature measured inside the shoe. The pumping cycle of the EHD occurs in four consecutive stages as it undergoes repeated loading and unloading inside the shoe. In stage 1, force applied during foot strike compresses the EHD and increases the pressure of the gas within the porous foam. When pressure inside the EHD exceeds that of the ESB, the outlet valve opens, releasing compressed air to the ESB for storage (stage 2). Stage 3 commences with liftoff of the foot; as the stepping force is removed, the EHD expands under the restoring force of the foam, and gas pressure inside the pouch falls. Last, in stage 4, fresh air is drawn in through the intake valve when the internal pressure drops below that of ambient air. The forces acting on the top wall of the pouch (represented by the "piston" of a pneumatic cylinder) at an arbitrary point during this cycle are shown in Fig. 2B; these include the stepping force  $F_{\text{step}}$  exerted by the foot, the restoring force  $F_{\text{spring}}$  from the foam, and the pressure forces  $F_{\text{atm}}$  and  $F_{\text{gas}}$ , respectively, resulting from internal and external air pressure acting on the effective contact area of the pouch.

Accurate modeling of the pressure within the EHD during the stepping cycle required realistic descriptions of the stepping force, pouch deformation, and reaction force from the foam. To this end, we measured the stepping force on the EHD during walking using force-sensing resistors mounted on the insole of the user's shoe (fig. S5). The transient force profile could be well approximated by a trapezoidal waveform with frequency equaling the rate of footfalls during walking (Fig. 2B); the peak force was inferred separately from measurements of the peak gas pressure attained during the compression phase. The flattening of the lenticular EHD pouch when compressed by the foot results in nonlinear changes in its internal volume and effective contact area; furthermore, the polyurethane foam behaves as a nonlinear spring, and its reaction force diverges upon approaching maximum deformation. The change in gas volume and the restoring force from the foam were both measured as a function of vertical displacement through simulated compression of the EHD using a universal testing machine (Instron 68SC-2); the

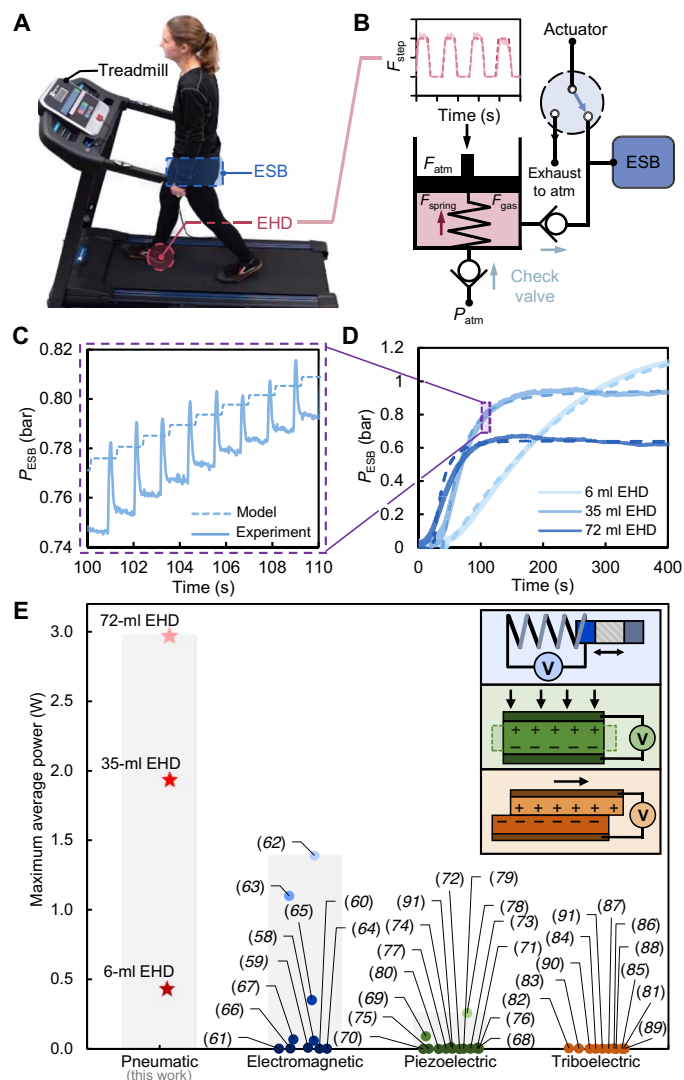


**Fig. 2. Characterizing the performance of the energy harvesting system.** (A) A user wearing the energy harvesting system walks on a treadmill during experimental measurements. (B) Schematic representation of the mechano-fluidic model used for performance evaluation and optimization. The inset shows the experimentally measured stepping force (solid curve) along with the matching trapezoidal waveform (dashed curve) used to model it. (C) Transient pressure traces predicted by the model (dashed curves) were validated against experimental measurements (solid curves). (D) Predicted and measured gas pressure inside the ESB for a 55-kg user walking at 3 mph. (E) Comparison of the maximum power output of the insole EHD with existing electromagnetic, piezoelectric, and triboelectric foot-strike energy harvesting systems.

internal volume of the EHD was approximated using a quadratic polynomial fit (fig. S4), whereas the foam reaction force showed good conformance to a neo-Hookean-type force function (fig. S6). We developed a time-stepping routine that solves the nonlinear force balance equation numerically to capture the temporal evolution of system parameters—such as the deformation of the EHD and the rate of airflow to the ESB—for any arbitrary choice of the stepping force. A detailed description of our model, including the executable code, is provided in the Supplementary Materials. The model predictions for the 6-, 35-, and 72-ml EHDs are shown

alongside experimental data in Fig. 2 (C and D); the predicted pressure traces show good agreement with the experimental pressure measurements for all three prototypes.

We used our mechano-fluidic model to determine the maximum average power (i.e., the maximum power that could be continuously supplied to a balanced load optimized for the system) and the overall energy conversion efficiency of our energy harvesting system. At any given pressure, the usable pneumatic energy stored in the ESB is given by the thermodynamic availability (exergy) of the compressed gas contained within it; the availability is equal to the maximum displacement work that can be extracted if the pressurized gas in the ESB is expanded reversibly against the atmosphere (eq. S24 and fig. S7A). To determine the average power output of the EHD, we divided the increase in stored energy during each foot strike by the duration of the corresponding step cycle (fig. S7B). For a 55-kg human user walking at 3 mph, our system achieved maximum average powers of 2.96, 1.94, and 0.44 W, respectively, using the 72-, 35-, and 6-ml EHDs (figs. S7B and S8). In Fig. 2E, we compare the maximum average power output of our system with those achieved by previously reported foot-strike energy harvesting systems based on piezoelectric, triboelectric, and electromagnetic mechanisms (38, 50). The comparison reveals that our system outperforms all approaches using electric mechanisms for energy harvesting by over 100% in maximum average power. Additional details on this comparison with extant foot strike energy harvesting systems are provided in the Supplementary Materials (table S6).

We define the conversion efficiency of our device as the ratio of the energy content of the ESB when it reaches full inflation (taken to be 99% of its final steady-state pressure; see fig. S9) to the cumulative mechanical work performed by the stepping force on the EHD until that point in time. The work input to the EHD was estimated by integrating the stepping force with respect to the displacement of the foot-pouch contact point; the negative work done by the EHD in raising the foot during the reinflation phase was ignored in this calculation, yielding conservative estimates of efficiency. Our optimized 6-ml EHD achieved an energy conversion efficiency of 23% (details are included in the Supplementary Materials).

### Validating system performance for different users and walking speeds

Figure 3A shows pneumatic energy harvesting using the 35-ml EHD for a 72-kg user walking at different speeds; whereas 3 mph (4.8 km/hour) serves as a typical speed for adults less than 30 years of age, a slower speed of about 1 mph (1.6 km/hour) may be more accessible for older individuals and users with mobility limitations. We observed that the frequency of footfalls (cadence) does not change substantially with the walking speed; the time interval between successive footfalls decreased only by about 30% (from 1.6 to 1.1 s) even with a threefold increase in speed (from 1 to 3 mph). Consequently, the rate of pressurization of the ESB was independent of speed, as indicated by the collapse of experimental pressure traces when normalized by the terminal ESB pressure (Fig. 3B). Furthermore, we observed only a slight (~10%) decrease in the maximum ESB pressure with a decrease in speed from 3 to 1 mph, which may be attributed to the known reduction in the amplitude of the stepping force at slower speeds (54). As neither the final pressure nor the fill rate is sensitive to changes in walking speed within the 1-to-3 mph range, we believe that our devices may be used effectively at reduced speeds with minimal to no modifications.

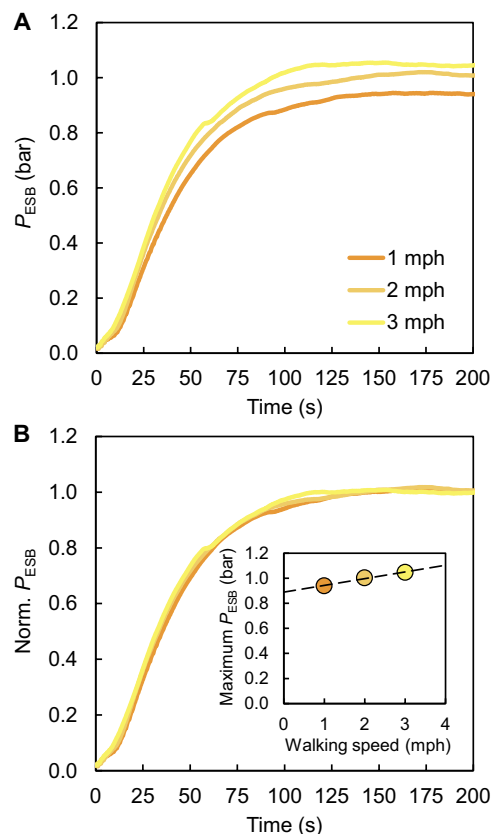


**Fig. 3. Effect of walking speed on energy harvesting performance.** (A) Evolution of ESB pressure with time for the 35-ml EHD and for a 72-kg human user walking at different speeds. Each curve represents transient pressure data smoothed over two step cycles and averaged over three replicate measurements. (B) The pressure traces in (A) collapse when normalized by the maximum ESB pressure, suggesting that the fill rate is independent of walking speed. The inset shows a small increase in the final gas pressure in the ESB at faster walking speeds.

We also tested the performance of the 35-ml EHD for five different users with body weights in the range of 52 to 87 kg (Fig. 4A), walking at a speed of 3 mph; results from these tests are shown in Fig. 4 (B and C). Neglecting small variations that may be attributed to inherent differences in foot size, shoe fit, cadence, and gait between users, we see that the final ESB pressure increases proportionally with the user's body weight on account of the increased maximum heel force exerted on the EHD. This conclusion is further corroborated by our mechano-fluidic model, which predicts a maximum ESB pressure that increases proportionally with the applied heel force (Fig. 4, D and E). Combining experimental trends (inset to Fig. 4C) with model predictions (Fig. 4E), we infer that approximately 61% of the users' bodyweight is transmitted via their heel to the EHD, which is in excellent agreement with data reported in the literature (54).

### Powering assistive actuators using harvested pneumatic energy

We demonstrated the ability of our energy harvesting system to generate sufficient energy to operate two pneumatic actuators made entirely of textiles: (i) an arm-lift assistive device (Fig. 5) and (ii) a supernumerary arm (Fig. 6), similar to devices reported in prior

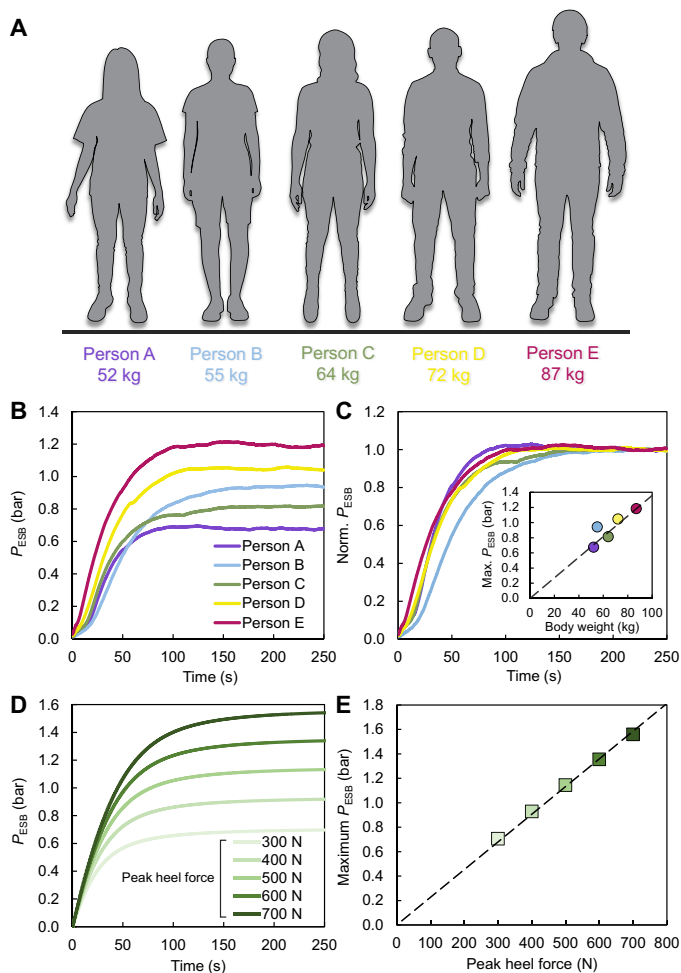


**Fig. 4. Evaluating system performance for users of different bodyweights.** (A) The cohort of test users representing a range of bodyweights, leg lengths, and foot sizes. (B) ESB pressure recorded as a function of time for the 35-ml EHD and for the five users all walking at 3 mph. Raw pressure data were smoothed over two step cycles and then averaged over three replicates. (C) Pressure traces in (B) normalized by the maximum ESB pressure show no notable variation in fill time between users. The inset indicates that the maximum ESB pressure increases proportionally with the user's bodyweight. (D) Transient responses of the mechano-fluidic model from a parametric sweep of the amplitude of stepping force, simulating users of different weights. (E) The final ESB pressure in (D) increases proportionally with the peak heel force exerted on the EHD.

work (25–27, 55). Both actuators were again fabricated by stacked laminate assembly of heat-sealable textiles in a process identical to that used for the EHD and ESB (figs. S2 and S3).

The arm-lift assistive device consists of a pneumatic bellows actuator (28, 56) made of six inflatable textile pouches sewn firmly beneath the shoulder of a long-sleeve compression shirt (Fig. 5A). When pressurized with air from the ESB, the actuator exerts a lifting torque at the shoulder to assist the user in raising (abducting) his or her arm (Fig. 5B). The number of pouches in the actuator determines the angle through which the arm is raised and the volume of air required per actuation cycle. To quantify the torque generated by the arm-lift device, we used a mannequin with a freely rotating shoulder joint to preclude all influences of muscular effort when testing on a human user. We varied the supply pressure and

the weight suspended from the arm (Fig. 5C) and measured the angle of rotation of the shoulder joint to infer the assistive torque (Fig. 5D). Our arm-lift actuator can apply a torque greater than 10 N m (table S7), which is consistent with the demands on current textile-based assistive devices (3). We also demonstrated the use of the arm-lift assistive device, powered solely by energy stored in the ESB, by a human user (Fig. 5A); a video showing the device in operation, on both the mannequin and the human user, is included as movie S2.

The supernumerary robotic arm (or “third arm”) operates using a dual-bladder system (Fig. 6A). The supporting bladder lends mechanical stiffness to the arm during use; it is mounted on the ESB and remains pressurized at all times. The actuating bladder forms the end effector of the arm and, when pressurized, allows the user to grasp and hold objects of various shapes. When not in use, the arm deflates to a compact size and folds conveniently out of the user's way (Fig. 6B). We tested our prototype robotic third arm by using it to grasp common household objects of various sizes, shapes, and weights, including a pair of scissors, a cup, and a granola bar (Fig. 6C and fig. S10); these demonstrations were performed solely using pressurized air generated by the energy harvesting system. Figure 6D shows a human user picking up a 42.6-g granola bar using the third arm and transporting it to the desired target location 1 m away. Figure 6E further demonstrates the utility of this device when the user's hands are full, enabling them to pick up and transport a piece of crumpled paper while also holding two large boxes. Operation of the third arm in this work is powered solely by energy harvested with the EHD and stored in the ESB; a video of these demonstrations is included as movie S3.

## DISCUSSION

This work demonstrates a soft, low-profile, and comfortable textile-based system that harvests energy during walking to operate pneumatic assistive and rehabilitative devices. A smaller EHD volume results in a slower fill rate but achieves a higher maximum pressure of air stored in the ESB; conversely, a larger EHD volume yields a faster fill rate but achieves a lower maximum pressure (fig. S9). This behavior occurs because the terminal ESB pressure is determined by the maximum pressure attained in the EHD; the latter, as per the force balance described by eq. S6, is set by the ratio of the net maximum force on the pouch wall (i.e., the peak heel force minus the spring force) to the effective contact area between the pouch and the foot. For a given heel force, therefore, a smaller EHD yields a higher maximum pressure due to the smaller contact area through which this force is exerted on the pouch wall. This inverse relationship between EHD size and maximum pressure is further corroborated by the predictions of our mechano-fluidic model, as seen in Fig. 2D. On the other hand, a larger EHD volume enables a faster fill rate on account of the greater quantity of gas pumped during each step cycle. The peak operating pressure and the rate of pressurization can be customized, respectively, by modifying the size of the EHD and the ESB, allowing fine-tuning of the energy harvesting system to meet the needs of the user. Our mechano-fluidic model simplifies device optimization by permitting exploration of the design space of possible EHD and ESB configurations before actual fabrication and testing. The textile-based energy harvesting system can thus be tailored, in principle, to support a variety of existing or future pneumatic actuators and soft wearables that users may need to support or augment their capabilities.

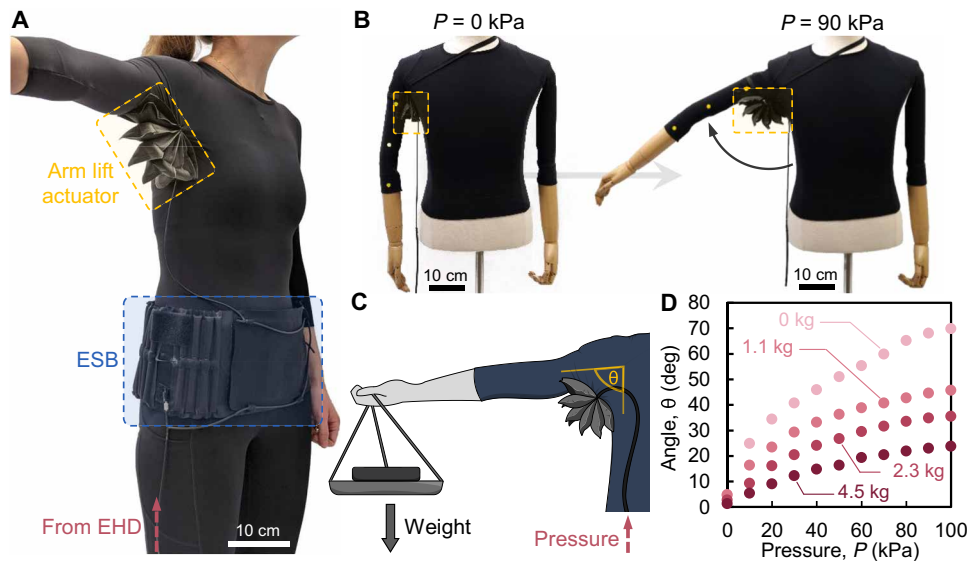


**Fig. 5. The pneumatic arm-lift assistive actuator.** (A) The actuator mounted on the user’s garment beneath the shoulder, shown in an actuated state after pressurization with compressed air generated by the user. (B) When pressurized, the actuator imparts a lifting torque on the shoulder joint of a mannequin; the mannequin was used to preclude any influence of muscular effort when testing on a human user. (C) Schematic representation of the experimental setup used to characterize the lifting torque. (D) The angular displacement of the arm produced by the actuator as a function of the input pressure and the weight suspended from the arm. Data markers denote averaged measurements, and the error bars indicate the range of observed angles across three replicates.

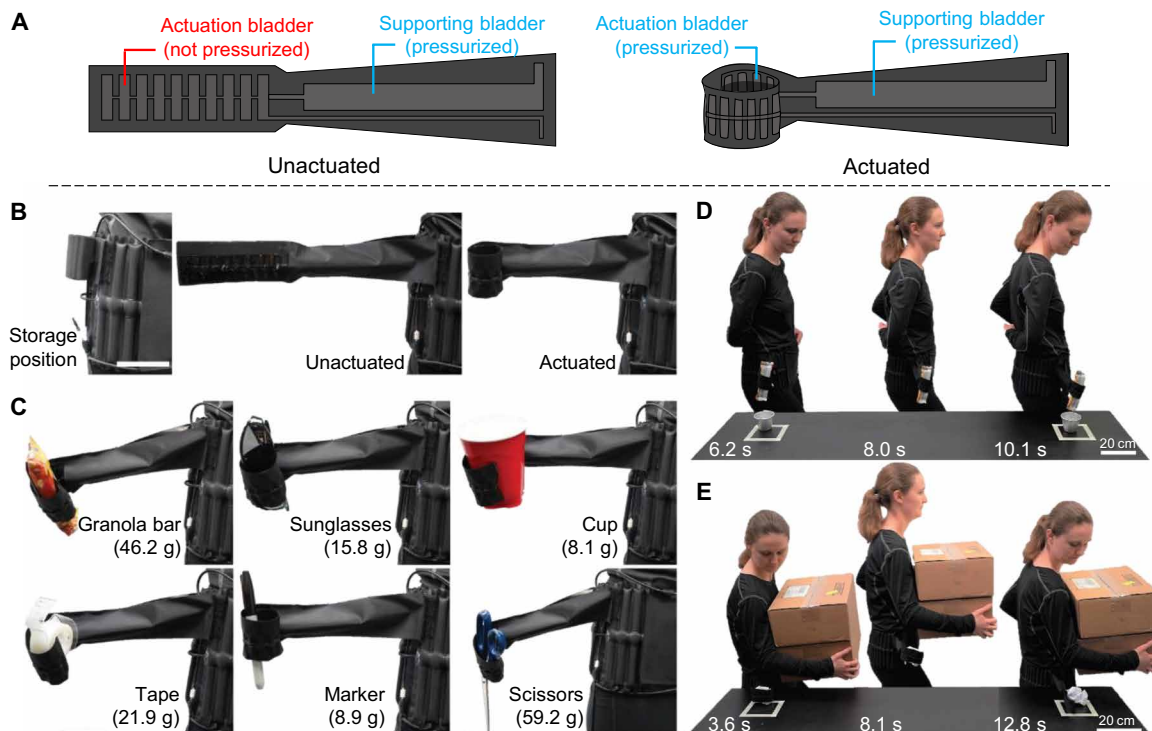


**Fig. 6. The supernumerary robotic arm powered by the energy harvesting system.** (A) Schematic diagram of the dual-bladder system that lends mechanical strength and enables gripper actuation. (B) The third arm in the storage, deployed (unactuated), and actuated configurations. (C) The third arm gripping objects of various shapes, weights, and surface textures. (D) A time-lapse sequence of the user using the third arm to pick up, transport, and deliver a 43-g granola bar. (E) The third arm used to pick up and transport a crumpled piece of paper while the user’s arms are full.

Our pneumatic energy harvesting system is not without limitations. For instance, the maximum energy that our device can supply in a single rapid draw is limited by the internal volume of the ESB. System capacity may be enhanced by enlarging the ESB or, more appropriately, by sizing the ESB commensurate with the maximum energy demand expected from various assistive actuators. For routine use, we envision sizing the components such that the ESB would enable several actuation cycles in quick succession before the user must wait for the EHD to replenish the expended gas. Although our system is well suited for powering pneumatic actuators directly, some users may still require actuators or controllers powered electrically, necessitating an onboard generator that runs on compressed air. Fortunately, this conversion step can be completed with an efficiency of approximately 50% (57), yielding a maximum average power output of about 1.5 W, which is still competitive with the maximum values reported for direct harvesting of electrical energy from walking (38).

All five users who tested our device reported that the EHD felt comfortable during walking, and most users found its firmness comparable to that of commercial insoles or shoe inserts. While the presence of the device inside the shoe was perceptible, none of the users reported discomfort, pain, or soreness after tests. A systematic investigation of user comfort and ergonomics will be helpful in guiding future optimization of our EHD design to minimize its influence on the user's gait and preclude any possibility of injury from long-term use. We believe that balancing user effort across the gait cycle by providing EHDs inside both shoes, as well as reshaping the EHDs to support the full area of each foot, will enhance both user comfort and the efficiency of our energy harvesting system. Another useful feature could be the provision of a valve to disconnect the EHD from the ESB, allowing the user to manually disable energy harvesting if desired.

In summary, the textile-based energy harvesting system developed in this work will support individuals with upper body functional limitations by powering assistive wearables that facilitate activities of daily living, thereby enabling improved quality of life and lowering barriers to social participation. An assessment of our system showed that it outperformed all other foot strike energy harvesting techniques relying on electric mechanisms by over 100% in maximum average power. During experiments, a maximum average power output of nearly 3 W was achieved, and an energy conversion efficiency of 23% was demonstrated. Our current system may be used directly by users with different walking speeds or body weights without design modification. Furthermore, our mechano-fluidic model—which we derived from first principles based on a fundamental thermodynamic and fluidic analysis of our system and validated against experimental results—allows further optimization of power, efficiency, and output characteristics to suit the needs of specific users. Our choice of structural materials, namely, heat-sealable textiles and foam, renders our devices soft, portable, and affordable, requiring only \$20 in materials to produce all wearable components. The fully assembled system weighs 140 g, which is less than 1/10th of the weight of the power and control infrastructure required to operate a similar textile-based supernumerary arm in prior work (25). Unlike expendable energy sources such as single-use battery packs, our device is capable of continuous power generation, eliminating the need for periodic replacement or refueling. In addition, the fabrication process is simple, inexpensive, and uses off-the-shelf textile materials and well-developed processes such as heat sealing

that may be readily scaled for mass production. We are therefore optimistic that our textile-based system can provide a lightweight, low-cost solution for powering wearable devices that will advance the state of the art beyond the limitations imposed by heavy and bulky power sources that serve the current generation of assistive and rehabilitative technologies.

## MATERIALS AND METHODS

### Experimental design

The goals of this work are twofold: (i) design a soft, wearable textile-based system for capturing pneumatic energy during walking and (ii) develop an accurate mechano-fluidic model, validated against experimental data, that can be used to predict and optimize system performance. We also demonstrated two textile-based assistive devices—an assistive device to aid shoulder motion and a supernumerary robotic arm—highlighting the ability of our system to meet the requirements of practical assistive and rehabilitative actuators for users with functional limitations. All our devices are textile-based with the goal of enabling a lightweight, unobtrusive, and comfortable wearable system. To allow scalability and facilitate replication of our work, we fabricated all devices from commercially available, inexpensive materials.

### Fabrication of the insole EHD

Three different EHD prototypes were fabricated with pouch volumes of 6, 35, and 72 ml; dimensions of the pouches were chosen to fit comfortably and unobtrusively inside the user's shoe. A desktop laser engraver (K40, Orion Motor Tech) was used to cut the outer layers of heat-sealable textile (FHST, TPU-coated nylon taffeta, Seattle Fabrics Inc.) and an inner layer of silicone-coated nonstick textile (FRC13, 1.3 oz. silicone-impregnated ripstop, Seattle Fabrics Inc.) as shown in Fig. 1A. The layers were stacked, aligned, and then heat sealed using a benchtop heat press (DK20SP, Geo Knight) at a temperature of 208°C and cylinder air pressure of 50 psi for a duration of 30 s. Next, a water-blown polyurethane foam mixture (FlexFoam-iT! X, Smooth-On) was prepared, and a premeasured quantity of the mixture, calibrated to achieve the intended pouch volume after expansion, was injected into the textile pouch using a syringe (Fig. 1A). The foam was allowed to expand to its final volume and fully cure over a period of at least 2 hours. Last, pneumatic connections were glued to the EHD using flexible rubber tubing (9776T1, McMaster-Carr), and check valves were added. The completed EHD is shown in Fig. 1B. Each of the three EHD prototypes weighed less than 27 g and cost less than \$3 to fabricate (even when estimated using retail prices; see table S1).

### Fabrication of the wearable ESB

The ESB was designed with an internal volume of approximately 744 ml, distributed across four bladder arrays that were pneumatically linked in series via soft rubber tubing (fig. S1). The textile bladders were formed by laser patterning and heat sealing TPU-coated nylon taffeta fabric by a process identical to that used for the EHD. A computerized sewing machine (SQ9285, Brother) was used to stitch the bladder array into a wearable belt by adding elastic as well as hook-and-loop (“Velcro”) attachments. Last, soft rubber tubing (9776T1, McMaster-Carr) was glued to the bladders to form pneumatic lines and to interconnect different sections of the bladder array. The completed ESB is shown in Fig. 1C; it weighed 91 g and

cost \$3 to fabricate (even when estimated using retail prices; see table S2).

The multibladder design of the ESB was specifically chosen to avoid pressure on the user's body during use; the hook-and-loop fasteners and elastic strips permit an adjustable and comfortable fit that accommodates users with different waist sizes, without restricting their range of motion or breathing. Once the bladders are fully inflated at ambient pressure, the ESB behaves as a constant volume tank; pressurization of the stored gas during walking causes no further lateral contraction of the bladders, precluding any feeling of constriction or discomfort to the user.

### Assembly of the energy harvesting system

Two miniature plastic check valves (C-116B-SI-PS, Industrial Specialties Manufacturing) were attached to the EHD to enable its pumping action. The valves were configured to permit unidirectional airflow either (i) from the atmosphere to the EHD or (ii) from the EHD to the ESB (Fig. 1C). We used soft and flexible EPDM rubber tubing (durometer hardness 60A, minimum bend radius less than ¼") to convey pressurized air from the outlet of the insole EHD to the inlet of the ESB (worn at the hip level) and from the ESB to various assistive devices. Tubes were routed along the user's garment using miniature hook and loop attachments to prevent kinking due to leg motion. User-controlled actuation of assistive devices was accomplished using a three-way valve (62475K42, Master-Carr) for inflating and deflating the pneumatic end effectors. The assembled system is shown in Fig. 1C; the overall system weighed 136 g and cost \$21 to fabricate (even when estimated using retail prices; see table S3).

### Fabrication of the arm-lift assistive device

The bellow actuator—consisting of six inflatable textile pouches—was formed by stacking and heat sealing 16 layers of TPU-coated nylon taffeta (FHST, Seattle Fabrics Inc.) interspersed with 13 layers of nonstick silicone-impregnated ripstop (FRC13, Seattle Fabrics Inc.), as shown in fig. S2. Heat sealing was performed using a benchtop heat press (DK20SP, Geo Knight) at a temperature of 200°C, cylinder pressure of 80 psi, and for a duration of 80 s. A computerized sewing machine (SQ9285, Brother) was then used to firmly attach the bellow actuator under the arm of a long-sleeve compression shirt (Fig. 3A and fig. S2). Last, soft rubber tubing (9776T1, McMaster-Carr) was glued to the device to provide pneumatic connection to the control valve. The arm-lift assistive device (including the compression shirt) weighed 113 g and cost less than \$23 to fabricate (even when estimated using retail prices; see table S4). For the experiment shown in Fig. 5C, we used a manual pressure regulator to vary the input pressure to the arm-lift and thereby modulate the angular displacement of the arm.

### Fabrication of the supernumerary robotic arm

We built two prototype third-arm devices—a 30-cm “long” version, as well as an 18-cm “short” version—each consisting of two inflatable textile bladders: one for support and the other for actuating the gripper. Figure 4 shows the long arm in operation, whereas additional results for the short arm are included in fig. S10. Both devices were made by heat sealing three layers each of TPU-coated nylon taffeta (FHST, Seattle Fabrics Inc.), interspersed with two layers each of nonstick silicone-impregnated ripstop (FRC13, Seattle Fabrics Inc.), as shown in fig. S3. Heat sealing was performed using a benchtop heat press (DK20SP, Geo Knight) at a temperature of

208°C, pressure of 60 psi, and for a duration of 40 s. A computerized sewing machine (SQ9285, Brother) was then used to add the textile frame supporting the cantilevered arm and to affix a loop attachment point to the wearable ESB (fig. S3). Separate pneumatic connections to the support and actuation bladders were made using soft rubber tubing (9776T1, McMaster-Carr). The actuating bladder was connected to the three-way valve for controlled actuation of the supernumerary arm, whereas the support bladder was directly fed from the ESB through a check valve (C-116B-SI-PS, Industrial Specialties Manufacturing) to prevent deflation during operation. Last, a thin layer of a soft and tacky elastomer (Ecoflex GEL, Smooth-On) was applied to the gripping surface of the arm to improve grip on objects with smooth and slippery surfaces. The short and long third arm devices weighed 9 and 14 g, respectively, and cost \$8 each to fabricate (table S5).

### Experimental evaluation of the performance of the energy harvesting system

Experimental measurements of system performance were conducted with users walking on a treadmill (TR150, Xterra Fitness). We tested our device with users of different body weights (52 to 87 kg), who were all authors of this work. Except for data shown in Fig. 3, tests were performed at a speed of 3 mph, corresponding to the average walking speed for users less than 30 years old (53) (Fig. 2A). For each test, the user walked on the treadmill at a steady pace until the wearable tank was fully inflated. The stepping force applied on the insole EHD during walking was recorded using a force-sensing resistor (FSR 406, Interlink Electronics) mounted inside the user's shoe and connected to a voltage divider circuit and an analog voltage acquisition system (USB-6211, National Instruments) as shown in fig. S5. The gas pressure at the inlet of the ESB was monitored using a pressure sensor (ADP5151, Panasonic), which was also connected to an analog data acquisition system (NI USB-6002, National Instruments).

### SUPPLEMENTARY MATERIALS

Supplementary material for this article is available at <https://science.org/doi/10.1126/sciadv.abo2418>

### REFERENCES AND NOTES

1. D. M. Taylor, Americans with disabilities: 2014. *Curr. Popul. Rep.*, 1–32 (2018).
2. I. M. Majer, W. J. Nusselder, J. P. Mackenbach, B. Klijns, P. H. M. van Baal, Mortality risk associated with disability: A population-based record linkage study. *Am. J. Public Health* **101**, e9–e15 (2011).
3. V. Sanchez, C. J. Walsh, R. J. Wood, Textile technology for soft robotic and autonomous garments. *Adv. Funct. Mater.* **31**, 2008278 (2021).
4. P. E. Dupont, B. J. Nelson, M. Goldfarb, B. Hannaford, A. Menciassi, M. K. O'Malley, N. Simaan, P. Valdastri, G.-Z. Yang, A decade retrospective of medical robotics research from 2010 to 2020. *Sci. Robot.* **6**, eabi8017 (2021).
5. C.-Y. Chu, R. M. Patterson, Soft robotic devices for hand rehabilitation and assistance: A narrative review. *J. Neuroeng. Rehabil.* **15**, 9 (2018).
6. P. Polygerinos, Z. Wang, K. C. Galloway, R. J. Wood, C. J. Walsh, Soft robotic glove for combined assistance and at-home rehabilitation. *Rob. Auton. Syst.* **73**, 135–143 (2015).
7. H. In, B. B. Kang, M. Sin, K.-J. Cho, Exo-glove: A wearable robot for the hand with a soft tendon routing system. *IEEE Robot. Autom. Mag.* **22**, 97–105 (2015).
8. G. Agarwal, M. A. Robertson, H. Sonar, J. Paik, Design and computational modeling of a modular, compliant robotic assembly for human lumbar unit and spinal cord assistance. *Sci. Rep.* **7**, 14391 (2017).
9. D. Govin, L. Saenz, G. Athanasaki, L. Snyder, P. Polygerinos, Design and Development of a Soft Robotic Back Orthosis, in *2018 Design of Medical Devices Conference* (American Society of Mechanical Engineers, 2018).
10. C. T. O'Neill, N. S. Phipps, L. Cappello, S. Paganoni, C. J. Walsh, A soft wearable robot for the shoulder: Design, characterization, and preliminary testing, in *2017 International Conference on Rehabilitation Robotics (ICORR)* (IEEE, 2017), pp. 1672–1678.



11. R. F. Natividad, C. H. Yeow, Development of a soft robotic shoulder assistive device for shoulder abduction, in *2016 6th IEEE International Conference on Biomedical Robotics and Biomechanics (BioRob)* (IEEE, 2016), pp. 989–993.
12. C. S. Simpson, A. M. Okamura, E. W. Hawkes, Exomuscle: An inflatable device for shoulder abduction support, in *2017 IEEE International Conference on Robotics and Automation (ICRA)* (IEEE, 2017), pp. 6651–6657.
13. T. H. Koh, N. Cheng, H. K. Yap, C.-H. Yeow, Design of a soft robotic elbow sleeve with passive and intent-controlled actuation. *Front. Neurosci.* **11**, 597 (2017).
14. V. Oguntosin, W. S. Harwin, S. Kawamura, S. J. Nasuto, Y. Hayashi, Development of a wearable assistive soft robotic device for elbow rehabilitation, in *2015 IEEE International Conference on Rehabilitation Robotics (ICORR)* (IEEE, 2015), pp. 747–752.
15. D. Chiaradia, M. Xiloyannis, C. W. Antuvan, A. Frisoli, L. Masia, Design and embedded control of a soft elbow exosuit, in *2018 IEEE International Conference on Soft Robotics (RoboSoft)* (IEEE, 2018), pp. 565–571.
16. J. Realmuto, T. Sanger, A robotic forearm orthosis using soft fabric-based helical actuators, in *2019 2nd IEEE International Conference on Soft Robotics (RoboSoft)* (IEEE, 2019), pp. 591–596.
17. S.-H. Park, J. Yi, D. Kim, Y. Lee, H. S. Koo, Y.-L. Park, A Lightweight, Soft Wearable Sleeve for Rehabilitation of Forearm Pronation and Supination, in *2019 2nd IEEE International Conference on Soft Robotics (RoboSoft)* (IEEE, 2019), pp. 636–641.
18. N. W. Bartlett, V. Lyau, W. A. Raiford, D. Holland, J. B. Gafford, T. D. Ellis, C. J. Walsh, A soft robotic orthosis for wrist rehabilitation, *ASME. J. Med. Devices* **9**, 030918 (2015).
19. D. Serrano, D.-S. Copaci, L. Moreno, D. Blanco, SMA based wrist exoskeleton for rehabilitation therapy, in *2018 IEEE/RSJ International Conference on Intelligent Robots and Systems (IROS)* (IEEE, 2018), pp. 2318–2323.
20. B. W. K. Ang, C.-H. Yeow, Design and characterization of a 3D printed soft robotic wrist sleeve with 2 DoF for stroke rehabilitation, in *2019 2nd IEEE International Conference on Soft Robotics (RoboSoft)* (IEEE, 2019), pp. 577–582.
21. M. A. Gull, S. Bai, T. Bak, A review on design of upper limb exoskeletons. *Robotics* **9**, 16 (2020).
22. S. Lessard, P. Pansodtee, A. Robbins, J. M. Trombadore, S. Kurniawan, M. Teodorescu, A soft exosuit for flexible upper-extremity rehabilitation. *IEEE Trans. Neural Syst. Rehabil. Eng.* **26**, 1604–1617 (2018).
23. P. H. Nguyen, C. Sparks, S. G. Nuthi, N. M. Vale, P. Polygerinos, Soft poly-limbs: Toward a new paradigm of mobile manipulation for daily living tasks. *Soft Robot.* **6**, 38–53 (2019).
24. P. H. Nguyen, I. B. Imran Mohd, C. Sparks, F. L. Arellano, W. Zhang, P. Polygerinos, fabric soft poly-limbs for physical assistance of daily living tasks, in *2019 International Conference on Robotics and Automation (ICRA)* (IEEE, 2019), pp. 8429–8435.
25. X. Liang, H. Cheong, C. K. Chui, C.-H. Yeow, A fabric-based wearable soft robotic limb. *J. Mech. Robot.* **11**, 031003 (2019).
26. X. Liang, H. K. Yap, J. Guo, R. C. H. Yeow, Y. Sun, C. K. Chui, Design and characterization of a novel fabric-based robotic arm for future wearable robot application, in *2017 IEEE International Conference on Robotics and Biomimetics (ROBIO)* (IEEE, 2017), pp. 367–372.
27. X. Liang, H. Cheong, Y. Sun, J. Guo, C. K. Chui, C.-H. Yeow, Design, characterization, and implementation of a two-DOF fabric-based soft robotic arm. *IEEE Robot. Autom. Lett.* **3**, 2702–2709 (2018).
28. C. M. Thalman, Q. P. Lam, P. H. Nguyen, S. Sridar, P. Polygerinos, A novel soft elbow exosuit to supplement bicep lifting capacity, in *2018 IEEE/RSJ International Conference on Intelligent Robots and Systems (IROS)* (IEEE, 2018), pp. 6965–6971.
29. F. A. Panizzolo, I. Galiana, A. T. Asbeck, C. Sivi, K. Schmidt, K. G. Holt, C. J. Walsh, A biologically-inspired multi-joint soft exosuit that can reduce the energy cost of loaded walking. *J. Neuroeng. Rehabil.* **13**, 43 (2016).
30. Y. Ding, F. A. Panizzolo, C. Sivi, P. Malcolm, I. Galiana, K. G. Holt, C. J. Walsh, Effect of timing of hip extension assistance during loaded walking with a soft exosuit. *J. Neuroeng. Rehabil.* **13**, 87 (2016).
31. M. Al-Sada, T. Höglund, M. Khamis, J. Urbani, T. Nakajima, Orochi: Investigating requirements and expectations for multipurpose daily used supernumerary robotic limbs, in *Proceedings of the 10th Augmented Human International Conference 2019* (ACM, New York, NY, USA, 2019), pp. 1–9.
32. B. Llorens-Bonilla, F. Parietti, H. H. Asada, Demonstration-based control of supernumerary robotic limbs, in *2012 IEEE/RSJ International Conference on Intelligent Robots and Systems (IROS)* (IEEE, 2012), pp. 3936–3942.
33. F. Wu, H. Asada, Supernumerary robotic fingers: An alternative upper-limb prosthesis, in *Volume 2: Dynamic Modeling and Diagnostics in Biomedical Systems; Dynamics and Control of Wind Energy Systems; Vehicle Energy Management Optimization; Energy Storage, Optimization; Transportation and Grid Applications; Estimation and Identification Method* (American Society of Mechanical Engineers, 2014), V002T16A009.
34. I. Hussain, G. Salvietti, G. Spagnoletti, M. Malvezzi, D. Cioncoloni, S. Rossi, D. Praticchizzo, A soft supernumerary robotic finger and mobile arm support for grasping compensation and hemiparetic upper limb rehabilitation. *Rob. Auton. Syst.* **93**, 1–12 (2017).
35. A. Rajappan, B. Jumet, D. J. Preston, Pneumatic soft robots take a step toward autonomy. *Sci. Robot.* **6**, eabg6994 (2021).
36. B. Jumet, M. D. Bell, V. Sanchez, D. J. Preston, A data-driven review of soft robotics. *Adv. Intell. Syst.* **4**, 2100163 (2021).
37. T. Starner, J. Paradiso, Human-generated power for mobile electronics, in *Low-Power Electronics Design*, C. Piguet, Ed. (CRC Press, 2004), chap. 45.
38. Y.-M. Choi, M. Lee, Y. Jeon, Wearable biomechanical energy harvesting technologies. *Energies* **10**, 1483 (2017).
39. H. Shi, Z. Liu, X. Mei, Overview of human walking induced energy harvesting technologies and its possibility for walking robotics. *Energies* **13**, 86 (2020).
40. F. A. Matulch, Foot actuated pressure generator. U.S. Patent 2,435,928 (1948).
41. S. R. Anton, H. A. Sodano, A review of power harvesting using piezoelectric materials (2003–2006). *Smart Mater. Struct.* **16**, R1–R21 (2007).
42. S. Niu, X. Wang, F. Yi, Y. S. Zhou, Z. L. Wang, A universal self-charging system driven by random biomechanical energy for sustainable operation of mobile electronics. *Nat. Commun.* **6**, 8975 (2015).
43. J. Chen, Y. Huang, N. Zhang, H. Zou, R. Liu, C. Tao, X. Fan, Z. L. Wang, Micro-cable structured textile for simultaneously harvesting solar and mechanical energy. *Nat. Energy* **1**, 16138 (2016).
44. J. He, C. Lu, H. Jiang, F. Han, X. Shi, J. Wu, L. Wang, T. Chen, J. Wang, Y. Zhang, H. Yang, G. Zhang, X. Sun, B. Wang, P. Chen, Y. Wang, Y. Xia, H. Peng, Scalable production of high-performing woven lithium-ion fibre batteries. *Nature* **597**, 57–63 (2021).
45. T. Shahid, D. Gouwanda, S. G. Nurzaman, A. A. Gopalai, Moving toward soft robotics: A decade review of the design of hand exoskeletons. *Biomimetics* **3**, 17 (2018).
46. P. Polygerinos, N. Correll, S. A. Morin, B. Mosadegh, C. D. Onal, K. Petersen, M. Cianchetti, M. T. Tolley, R. F. Shepherd, Soft robotics: Review of fluid-driven intrinsically soft devices; manufacturing, sensing, control, and applications in human-robot interaction. *Adv. Eng. Mater.* **19**, 1700016 (2017).
47. D. J. Preston, P. Rothmund, H. J. Jiang, M. P. Nemitz, J. Rawson, Z. Suo, G. M. Whitesides, Digital logic for soft devices. *Proc. Natl. Acad. Sci. U.S.A.* **116**, 7750–7759 (2019).
48. D. J. Preston, H. J. Jiang, V. Sanchez, P. Rothmund, J. Rawson, M. P. Nemitz, W. Lee, Z. Suo, C. J. Walsh, G. M. Whitesides, A soft ring oscillator. *Sci. Robot.* **4**, eaaw5496 (2019).
49. K. Ogawa, C. Thakur, T. Ikeda, T. Tsuji, Y. Kurita, Development of a pneumatic artificial muscle driven by low pressure and its application to the unplugged powered suit. *Adv. Robot.* **31**, 1135–1143 (2017).
50. K. Ogawa, T. Ikeda, Y. Kurita, Unplugged powered suit for superhuman tennis, in *2018 12th France-Japan and 10th Europe-Asia Congress on Mechatronics* (IEEE, 2018), pp. 361–364.
51. I. Jones, The use of heat sealing, hot air and hot wedge to join textile materials, in *Joining Textiles*, I. Jones, G. K. Stylios, Eds. (Woodhead Publishing, 2013), chap. 11, pp. 355–373.
52. R. S. Diteasawat, T. Helps, M. Taghavi, J. Rossiter, Electro-pneumatic pumps for soft robotics. *Sci. Robot.* **6**, eabc3721 (2021).
53. M. Schimpl, C. Moore, C. Lederer, A. Neuhaus, J. Sambrook, J. Danesh, W. Ouweland, M. Daumer, Association between walking speed and age in healthy, free-living individuals using mobile accelerometry—A cross-sectional study. *PLOS ONE* **6**, e23299 (2011).
54. P. R. Cavanagh, M. M. Rodgers, A. Liboshi, Pressure distribution under symptom-free feet during barefoot standing. *Foot Ankle* **7**, 262–278 (1987).
55. J. Fang, J. Yuan, M. Wang, L. Xiao, J. Yang, Z. Lin, P. Xu, L. Hou, Novel accordion-inspired foldable pneumatic actuators for knee assistive devices. *Soft Robot.* **7**, 95–108 (2020).
56. P. H. Nguyen, W. Zhang, Design and computational modeling of fabric soft pneumatic actuators for wearable assistive devices. *Sci. Rep.* **10**, 9638 (2020).
57. D. Krähenbühl, C. Zwysig, H. Weser, J. W. Kolar, Theoretical and experimental results of a mesoscale electric power generation system from pressurized gas flow. *J. Micromech. Microeng.* **19**, 094009 (2009).
58. J. Hayashida, thesis, Massachusetts Institute of Technology (2000).
59. M. Duffy, D. Carroll, Electromagnetic generators for power harvesting, in *2004 IEEE 35th Annual Power Electronics Specialists Conference (IEEE Cat. No.04CH37551)* (IEEE, 2004), pp. 2075–2081.
60. Y. Rao, S. Cheng, D. P. Arnold, An energy harvesting system for passively generating power from human activities. *J. Micromech. Microeng.* **23**, 114012 (2013).
61. J.-X. Shen, C.-F. Wang, P. C.-K. Luk, D.-M. Miao, D. Shi, C. Xu, A shoe-equipped linear generator for energy harvesting. *IEEE Trans. Ind. Appl.* **49**, 990–996 (2013).
62. L. Xie, M. Cai, An in-shoe harvester with motion magnification for scavenging energy from human foot strike. *IEEE/ASME Trans. Mechatron.* **20**, 3264–3268 (2015).
63. A. M. Purwadi, S. Parasuraman, M. K. A. A. Khan, I. Elamvazuthi, Development of biomechanical energy harvesting device using heel strike. *Procedia Comput. Sci.* **76**, 270–275 (2015).
64. K. Ylli, D. Hoffmann, A. Willmann, P. Becker, B. Folkmer, Y. Manoli, Energy harvesting from human motion: Exploiting swing and shock excitations. *Smart Mater. Struct.* **24**, 025029 (2015).
65. L. Xie, J. Li, S. Cai, X. Li, Design and experiments of a self-charged power bank by harvesting sustainable human motion. *Adv. Mech. Eng.* **8**, 168781401665137 (2016).

66. S. Wu, P. C. K. Luk, C. Li, X. Zhao, Z. Jiao, Y. Shang, An electromagnetic wearable 3-DoF resonance human body motion energy harvester using ferrofluid as a lubricant. *Appl. Energy* **197**, 364–374 (2017).
67. Z. Li, X. Jiang, Y. Peng, J. Luo, S. Xie, H. Pu, Design and experimental studies of a heel-embedded energy harvester for self-powered wearable electronics, in *ASME 2021 Conference on Smart Materials, Adaptive Structures and Intelligent Systems* (American Society of Mechanical Engineers, 2021), V001T04A006.
68. N. S. Shenck, J. A. Paradiso, Energy scavenging with shoe-mounted piezoelectrics. *IEEE Micro* **21**, 30–42 (2001).
69. C. A. Howells, Piezoelectric energy harvesting. *Energy. Conver. Manage.* **50**, 1847–1850 (2009).
70. J. G. Rocha, L. M. Goncalves, P. F. Rocha, M. P. Silva, S. Lanceros-Mendez, Energy harvesting from piezoelectric materials fully integrated in footwear. *IEEE Trans. Ind. Electron.* **57**, 813–819 (2010).
71. J. Zhao, Z. You, A shoe-embedded piezoelectric energy harvester for wearable sensors. *Sensors* **14**, 12497–12510 (2014).
72. R. Meier, N. Kelly, O. Almog, P. Chiang, A piezoelectric energy-harvesting shoe system for podiatric sensing, in *2014 36th Annual International Conference of the IEEE Engineering in Medicine and Biology Society* (IEEE, 2014), pp. 622–625.
73. W.-S. Jung, M.-J. Lee, M.-G. Kang, H. G. Moon, S.-J. Yoon, S.-H. Baek, C.-Y. Kang, Powerful curved piezoelectric generator for wearable applications. *Nano Energy* **13**, 174–181 (2015).
74. H. Kalantarian, M. Sarrafzadeh, Pedometers without batteries: An energy harvesting shoe. *IEEE Sens. J.* **16**, 8314–8321 (2016).
75. K. Fan, Z. Liu, H. Liu, L. Wang, Y. Zhu, B. Yu, Scavenging energy from human walking through a shoe-mounted piezoelectric harvester. *Appl. Phys. Lett.* **110**, 143902 (2017).
76. A. C. Turkmen, C. Celik, Energy harvesting with the piezoelectric material integrated shoe. *Energy* **150**, 556–564 (2018).
77. P. Chaudhary, P. Azad, Energy harvesting using shoe embedded with piezoelectric material. *J. Electron. Mater.* **49**, 6455–6464 (2020).
78. M. Ramalingam, E. Chinnavan, R. Puvirasi, N. H. Yu, Assistive technology for harvesting footstep energy in IoT enabled Smart shoe for the visually impaired, in *2021 International Conference on Software Engineering & Computer Systems and 4th International Conference on Computational Science and Information Management (ICSECS-ICOCSIM)* (IEEE, 2021), pp. 115–118.
79. N. Wang, R. Daniels, L. Connelly, M. Sotzing, C. Wu, R. Gerhard, G. A. Sotzing, Y. Cao, All-organic flexible ferroelectret nanogenerator with fabric-based electrodes for self-powered body area networks. *Small* **17**, 2103161 (2021).
80. S. Y. Jeong, L. L. Xu, C. H. Ryu, A. Kumar, S. Do Hong, D. H. Jeon, J. Y. Cho, J. H. Ahn, Y. H. Joo, I. W. Jeong, W. S. Hwang, T. H. Sung, Wearable shoe-mounted piezoelectric energy harvester for a self-powered wireless communication system. *Energies* **15**, 237 (2022).
81. T.-C. Hou, Y. Yang, H. Zhang, J. Chen, L.-J. Chen, Z. Lin Wang, Triboelectric nanogenerator built inside shoe insole for harvesting walking energy. *Nano Energy* **2**, 856–862 (2013).
82. K. Zhang, X. Wang, Y. Yang, Z. L. Wang, Hybridized electromagnetic–triboelectric nanogenerator for scavenging biomechanical energy for sustainably powering wearable electronics. *ACS Nano* **9**, 3521–3529 (2015).
83. T. Huang, C. Wang, H. Yu, H. Wang, Q. Zhang, M. Zhu, Human walking-driven wearable all-fiber triboelectric nanogenerator containing electrospun polyvinylidene fluoride triboelectric nanofibers. *Nano Energy* **14**, 226–235 (2015).
84. R. I. Haque, P.-A. Farine, D. Briand, Fully casted soft power generating triboelectric shoe insole. *J. Phys. Conf. Ser.* **773**, 012097 (2016).
85. R. I. Haque, P.-A. Farine, D. Briand, Soft triboelectric generators by use of cost-effective elastomers and simple casting process. *Sens. Actuators A Phys.* **271**, 88–95 (2018).
86. Y. Yun, S. Jang, S. Cho, S. H. Lee, H. J. Hwang, D. Choi, Exo-shoe triboelectric nanogenerator: Toward high-performance wearable biomechanical energy harvester. *Nano Energy* **80**, 105525 (2021).
87. W. Yuan, C. Zhang, B. Zhang, X. Wei, O. Yang, Y. Liu, L. He, S. Cui, J. Wang, Z. L. Wang, Wearable, breathable and waterproof triboelectric nanogenerators for harvesting human motion and raindrop energy. *Adv. Mater. Technol.* **7**, 2101139 (2022).
88. X. Wang, W. Tong, Y. Li, Z. Wang, Y. Chen, X. Zhang, X. Wang, Y. Zhang, Mica-based triboelectric nanogenerators for energy harvesting. *Appl. Clay Sci.* **215**, 106330 (2021).
89. X. Yao, A flexible triboelectric nanogenerator based on soft foam for rehabilitation monitor after foot surgery. *Mater. Technol.* **37**, 1516–1522 (2022).
90. Y. Gao, Z. Li, B. Xu, M. Li, C. Jiang, X. Guan, Y. Yang, Scalable core–spun coating yarn-based triboelectric nanogenerators with hierarchical structure for wearable energy harvesting and sensing via continuous manufacturing. *Nano Energy* **91**, 106672 (2022).
91. D. W. Lee, D. G. Jeong, J. H. Kim, H. S. Kim, G. Murillo, G.-H. Lee, H.-C. Song, J. H. Jung, Polarization-controlled PVDF-based hybrid nanogenerator for an effective vibrational energy harvesting from human foot. *Nano Energy* **76**, 105066 (2020).

**Acknowledgments:** Scanning electron micrographs in Fig. 1 were obtained at the Shared Equipment Authority at Rice University. This material is based upon work supported by the NSF under grant no. CMMI-2144809 and the NSF Graduate Research Fellowship Program under grant no. 1842494. **Funding:** This work was funded by the U.S. Coast Guard Advanced Education Program (R.A.S.), the Rice University Academy of Fellows Program (A.R.), NSF grant no. CMMI-2144809 (T.F.Y. and D.J.P.), NASA Space Technology Graduate Research Opportunity Award 80NSSC21K1276 (M.D.B.), NSF Graduate Research Fellowship grant no. 1842494 (B.J.), the National GEM Consortium GEM Fellowship (M.D.B. and V.S.), and a National Defense Science and Engineering Graduate Fellowship (V.S.). **Author contributions:** Conceptualization: R.A.S., A.R., V.S., and D.J.P. Data curation: R.A.S., A.R., T.F.Y., and D.J.P. Formal analysis: R.A.S., A.R., and D.J.P. Methodology: R.A.S., A.R., T.F.Y., Z.L., and D.J.P. Investigation: R.A.S., A.R., T.F.Y., Z.L., M.D.B., B.J., V.S., and D.J.P. Visualization: R.A.S., A.R., T.F.Y., Z.L., and D.J.P. Software: R.A.S., A.R., and D.J.P. Project administration: R.A.S. and D.J.P. Validation: R.A.S., A.R., and D.J.P. Supervision: D.J.P. Writing (original draft): R.A.S., A.R., and D.J.P. Writing (review and editing): R.A.S., A.R., T.F.Y., Z.L., M.D.B., B.J., V.S., and D.J.P. **Competing interests:** The authors declare that they have no competing interests. **Data and materials availability:** All data needed to evaluate the conclusions in the paper are present in the paper and/or the Supplementary Materials.

Submitted 22 January 2022

Accepted 12 July 2022

Published 24 August 2022

10.1126/sciadv.abo2418